

Quasiparticle relaxation dynamics in superconductors with different gap structures: theory and experiments on $\text{YBa}_2\text{Cu}_3\text{O}_{7-\delta}$

V.V.Kabanov, J. Demsar, B. Podobnik, D.Mihailovic
Jozef Stefan Institute, Jamova 39, Ljubljana, Slovenia

Photoexcited quasiparticle relaxation dynamics are investigated in a $\text{YBa}_2\text{Cu}_3\text{O}_{7-\delta}$ superconductor as a function of doping δ and temperature T using ultrafast time-resolved optical spectroscopy. A model calculation is presented which describes the temperature dependence of the photoinduced quasiparticle population n_{pe} , photoinduced transmission $|\Delta\mathcal{T}/\mathcal{T}|$ and relaxation time τ for three different superconducting gaps: (i) a temperature-dependent collective gap such that $\Delta(T) \rightarrow 0$ as $T \rightarrow T_c$, (ii) a temperature-*independent* gap, which might arise for the case of a superconductor with pre-formed pairs and (iii) an anisotropic (e.g. d -wave) gap with nodes. Comparison of the theory with data of photoinduced transmission $|\Delta\mathcal{T}/\mathcal{T}|$, reflection $|\Delta\mathcal{R}/\mathcal{R}|$ and quasiparticle recombination time τ in $\text{YBa}_2\text{Cu}_3\text{O}_{7-\delta}$ over a very wide range of doping ($0.1 < \delta < 0.48$) is found to give good quantitative agreement with a temperature-*dependent* BCS-like isotropic gap near optimum doping ($\delta < 0.1$) and a temperature-*independent* isotropic gap in underdoped $\text{YBa}_2\text{Cu}_3\text{O}_{7-\delta}$ ($0.15 < \delta < 0.48$). A pure d -wave gap was found to be inconsistent with the data.

I. INTRODUCTION

Ultrafast optical time resolved experiments performed on high- T_c superconductors in recent years have shown that a substantial transient change of the optical transmission or reflection can be induced in these materials by ultrashort laser pulse photoexcitation (PE). What makes these studies particularly interesting is the fact that in optimally doped superconductors where T_c is a maximum, the amplitude of the observed photoinduced transmission signal, $|\Delta\mathcal{T}/\mathcal{T}|$, (or reflection $|\Delta\mathcal{R}/\mathcal{R}|$) appears to increase dramatically below T_c^{1-4} . Furthermore, recently it was found that in underdoped $\text{YBa}_2\text{Cu}_3\text{O}_{7-\delta}$ ($\delta > 0.15$), the increase in amplitude could not be correlated with T_c , but rather with the so-called "pseudogap" temperature T^* which increases with increasing δ^5 . These observations together suggest rather strongly that the photoinduced effects are related to the opening of a gap (or pseudogap) in the density of states close to the Fermi energy. For optimally doped cuprate superconductors - on which most experiments were done so far - there has been substantial agreement in the literature regarding the experimental data. However, various groups have proposed very different explanations for the observed effects^{1,3,4,6} and their origin have remained controversial⁷.

In this paper we present a calculation of the photoinduced optical response in a superconductor for weak excitation and compare our results with systematic experimental data on $\text{YBa}_2\text{Cu}_3\text{O}_{7-\delta}$ as a function of δ and T . We derive expressions for the temperature dependence of the photoexcited quasiparticle density n_{pe} and photoinduced transmission amplitude $|\Delta\mathcal{T}/\mathcal{T}|$ for different possible gaps (or pseudogaps) which might be applicable to high- T_c cuprates. The simplest case considered is that of a gap, whose temperature dependence is mean-field like and is approximated using a BCS function. The second case considered is for a temperature-independent "pseudogap" which is relevant for a superconductor where condensation of pre-formed pairs into a superconducting state occurs at T_c but pairing takes place above this temperature. In this case the gap is not due to a collective effect, but essentially represents the pair binding energy E_B and is - to first approximation - temperature independent. Finally we discuss the case of an anisotropic gap with nodes, such as one might expect for a d -wave superconductor. In section V we present a calculation of the temperature dependence of the quasiparticle relaxation rate τ . Comparisons of the theoretical predictions with experimental data are made in each case and a detailed discussion is given in section VI.

II. EXPERIMENTAL DETAILS

The time-resolved experiments were performed using 100 fs, 800 nm pulses from a Ti:sapphire laser using single high frequency modulation of the pump at 200 kHz. The $\text{YBa}_2\text{Cu}_3\text{O}_{7-\delta}$ thin film samples were grown on MgO or SrTiO₃ substrates and annealed in oxygen to obtain different O concentrations δ . The T_c was measured by measuring the AC susceptibility in each case. The transition widths, defined as the temperature where χ drops to 90% of full diamagnetism, were typically 1-2 K for the $\delta < 0.15$ and 4-7 K for $\delta > 0.15$. The oxygen concentration was determined from T_c , which brings in some uncertainty near optimum doping, since the optimum T_c for YBCO is 90 K on SrTiO₃ substrates and 89 K on MgO substrates, which is 2-3 K lower than in single crystals. The typical film thicknesses were 100-120 nm and all experiments were performed in transmission through the sample. The typical energy of the laser pulse is 0.2 nJ, and the laser spot size typically 100 μm in diameter. In estimating the carrier density, the absorption

length was assumed to be $l \simeq 0.1 \mu\text{m}$. The CW temperature rise of the superconductor film due to laser heating was calibrated using a $30\mu\text{m}$ YBCO superconducting microbridge from the same batch and on the same substrate as in the optical experiments by measuring the change in resistivity with a 4-probe contact method. This temperature offset was then taken into account in the plots shown in Figures 1-6. The error in the sample temperature is thus reduced to less than $\pm 2 \text{ K}$.

The photoinduced transmission $|\Delta\mathcal{T}/\mathcal{T}|$ through two different films with $T_c = 90$ and 53 K respectively is shown in Fig. 1 at different temperatures above and below T_c . There are two decay components in each case, a fast component with $\tau \sim 0.3 - 2 \text{ ps}$, and a longer-lived component with $\tau_L > 10 \text{ ns}$, which appears as a nearly flat background already discussed elsewhere⁴. The latter will not be analysed here, except that it will be taken into account in the fitting procedure. The time-evolution of the traces was fitted (shown by the solid lines in Fig.1) using a model with a *single* exponential decay and a Gaussian temporal profile pump pulse, from which the amplitude of the photoinduced transmission, $|\Delta\mathcal{T}/\mathcal{T}|$, and relaxation time of the fast component, τ , was determined. The temperature dependence of $|\Delta\mathcal{T}/\mathcal{T}|$ and τ derived from the fits are plotted in Figs. 2, 4 and 5 and will be discussed together with the theory in the following sections.

III. INITIAL PHOTOEXCITED CARRIER RELAXATION

The initial phase of PE carrier relaxation after absorption of a pump laser photon proceeds very rapidly. After the laser pulse excites an electron-hole pair, these PE carriers thermalize among themselves with a characteristic time of $\tau_{e-e} \sim \frac{\hbar E_F}{2\pi E^2}$, where E is the carrier energy measured from the Fermi energy E_F . In this thermalization process, quasiparticle avalanche multiplication due to electron-electron collisions takes place as long as τ_{e-e} is less than the electron-phonon ($e\text{-}ph$) relaxation time τ_{e-ph} . Electron-phonon relaxation becomes important when the quasiparticle (QP) energy is reduced to $E = \sqrt{\frac{\hbar E_F}{2\pi\tau_{e-ph}}} \simeq 30 - 50 \text{ meV}$ (assuming $E_F \simeq 0.1 - 0.2 \text{ eV}$). τ_{e-ph} has been determined experimentally for the case of a $\text{YBa}_2\text{Cu}_3\text{O}_{7-\delta}$ ⁸ as well as $\text{Bi}_2\text{Sr}_2\text{CaCu}_2\text{O}_{8+x}$ and $\text{Bi}_2\text{Sr}_2\text{Ca}_2\text{Cu}_3\text{O}_{10+x}$ ⁹ from relaxation time fits in time resolved experiments using intense laser pulses. Using Allen's formula¹⁰ the $e\text{-}ph$ relaxation time for YBCO has been found to be $\tau_{e-ph} = \frac{T_e}{3\lambda\langle\omega^2\rangle} \simeq 100 \text{ fs}$ for initial carrier temperatures $T_e = E_I/C_e$ in the range 3000 K ⁸ and $\tau_{e-ph} \simeq 60 \text{ fs}$ for $T_e \simeq 410 \text{ K}$ ⁹. Here E_I is the energy density per unit volume deposited by the laser pulse, C_e is the electronic specific heat, λ is a constant which characterizes the electron-phonon interaction and $\langle\omega^2\rangle$ is a mean-square phonon frequency. λ has been determined from these experiments to be in the range $0.9 < \lambda < 1$ both in $\text{YBa}_2\text{Cu}_3\text{O}_{7-\delta}$ and $\text{Bi}_2\text{Sr}_2\text{CaCu}_2\text{O}_{8+x}$ superconductors. In experiments which we are considering here^{1,4,5}, the laser intensities are significantly smaller, and the photoexcited electronic temperature T_e is only few K in excess of the lattice temperature, i.e. $T_e \simeq T$, which gives an $e\text{-}ph$ relaxation time $\tau_{e-ph} \simeq 10 \text{ fs}$. Under these near-equilibrium conditions where the carrier temperature is near the lattice temperature, this value of τ_{e-ph} can be compared to the relaxation time determined from infrared reflectivity measurements. For energies of the order of $30 - 50 \text{ meV}$, $\hbar/\tau \sim 3000 \text{ cm}^{-1}$ ($\tau \sim 16 \text{ fs}$)¹¹ in good agreement with the estimated $\tau_{e-ph} \simeq 10 \text{ fs}$. In the absence of a gap in the low-energy density of states, this is the timescale of the electron -phonon thermalization.

In the presence of the gap the situation is strongly modified and a bottleneck in the relaxation occurs after $t \geq 10 \text{ fs}$. As a result QPs accumulate near the gap, forming a non-equilibrium distribution. Each photon thus creates $30 \sim 40$ QPs given by $E_{\text{pump}}/2\Delta$, where $E_{\text{pump}} = 1.5 \text{ eV}$ is the laser pump photon energy and 2Δ is the energy gap. Because the final relaxation step across the gap is strongly suppressed^{12,13} the QPs together with high frequency phonons (with $\hbar\omega > 2\Delta$) form a near-steady state distribution. The QP recombination dynamics of this system is governed by the emission and reabsorption of high frequency phonons. Phonons with $\hbar\omega < 2\Delta$ do not participate in the direct relaxation of the QPs, since in this case the QP final states would lie in the gap. (A quantitative justification for the assumption that phonons play a dominant role in the QP relaxation will be given in section V.) The basis for these pump-probe experiments is that this near-equilibrium QP population can be very effectively probed using excited state absorption using a suitable second optical probe pulse, giving direct information on QP dynamics and the nature of the gap itself.

Since the probe laser photon energy E_{probe} is typically *well above* the plasma frequency in high- T_c superconductors, we make the approximation that the transition probability for the probe light is given by the Fermi golden rule, with photoinduced quasiparticles as initial states and with final unoccupied states well above the Fermi energy in a band which lies approximately at $E_0 \sim E_{\text{probe}}$. The amplitude of the photoinduced absorption (PA) $|\Delta\mathcal{A}/\mathcal{A}|$ is then proportional to the photoinduced transmission $|\Delta\mathcal{T}/\mathcal{T}|$ (and in the linear approximation also to $|\Delta\mathcal{R}/\mathcal{R}|$) which is in turn proportional to the number of photoexcited quasiparticles n_{pe} . The probe signal is thus weighted by the O-Cu charge-transfer dipole matrix element and the joint DOS, so $|\Delta\mathcal{T}/\mathcal{T}| \propto -n_{pe}\rho_f |M_{ij}|^2$ where n_{pe} is the photoexcited carrier density, ρ_f is the final density of unoccupied states and $M_{ij} = \langle \mathbf{p} \cdot \mathbf{A} \rangle$ is the dipole matrix element. Although

recent experiments on $\text{YBa}_2\text{Cu}_3\text{O}_{7-\delta}$ with different E_{probe} show the existence of a resonance for $E_{\text{probe}} \sim 1.5$ eV⁴, we assume here that the adiabatic approximation can be applied, so the photoinduced carriers do not cause any change in ρ_f or M_{ij} . In this case the effect of the 1.5 eV resonance is to significantly enhance the sensitivity of the probe.

IV. TEMPERATURE DEPENDENCE OF THE QUASIPARTICLE DENSITY

A. Isotropic gap.

In discussing the theoretical explanation for the observed effects, it is important to make the distinction between experiments *(i)* in which the photoexcited charge carrier density is substantially less than the normal state carrier density, $n_{pe} \ll n_c$ so the laser makes only a weak perturbation on the superconductor^{1,4,5} and *(ii)* those where $n_{pe} \sim n_c$ and photoexcitation is sufficiently strong to close the superconducting gap^{2,3}. Whereas for the latter case *(ii)*, a theoretical description was proposed by Mazin⁶, so far there has been no theoretical calculation for the photoinduced effects in a superconductor for the case of weak photoexcitation *(i)*. The number of photogenerated quasiparticles in low-excitation density experiments is $n_{pe} \lesssim 3 \times 10^{-3}/\text{unit cell}$ ^{1,4,5}. On the other hand, the typical quasiparticle concentration in a high- T_c superconductor is $n_0 = 2N(0)\Delta \simeq 0.2 - 0.4/\text{unit cell}$, where $N(0)$ is the density of states at E_F . The number of photoexcited QPs is small compared to the normal state density $n_{pe}/n_0 \lesssim 10^{-2}$, so the weak photoexcitation approximation is clearly justified and the photoexcited quasiparticles make only a small perturbation of the distribution functions. Assuming that the energy gap is more or less isotropic (no nodes), we can approximate nonequilibrium phonon (n_{ω_q}) and quasiparticle (f_ϵ) distribution functions as follows¹⁴:

$$n_{\omega_q} = \begin{cases} \frac{1}{\exp(\frac{\hbar\omega_q}{k_B T}) - 1} & \hbar\omega_q < 2\Delta \\ \frac{1}{\exp(\frac{\hbar\omega_q}{k_B T'}) - 1} & \hbar\omega_q > 2\Delta \end{cases} \quad (1)$$

$$f_\epsilon = \frac{1}{\exp(\frac{\epsilon}{k_B T'}) + 1} \quad (2)$$

where T is the lattice temperature and T' is the temperature of quasiparticles and high frequency phonons with $\hbar\omega_q > 2\Delta$.

We can calculate n_{pe} using Eqs.(1), (2) and by considering the conservation of energy. Assuming Δ is temperature *independent* and large in comparison to T , the conservation of energy has the following form:

$$(n_{T'} - n_T) \Delta + (n_{T'}^2 - n_T^2) \frac{\nu \Delta}{2\hbar\Omega_c N(0)^2 k_B T'} = \mathcal{E}_I \quad (3)$$

here $n_{T'}$, n_T is the number of thermally excited quasiparticles per unit cell at T' and T respectively, \mathcal{E}_I is the energy density per unit cell deposited by the incident laser pulse, Ω_c is phonon frequency cut off and ν is the effective number of phonon modes per unit cell participating in the relaxation. Taking into account that $n_{pe} = (n_{T'} - n_T) \ll n_T$ and assuming that $n_T = 2N(0)k_B T \exp(-\Delta/k_B T)$, the number of photogenerated quasiparticles at temperature T is given by:

$$n_{pe} = \frac{\mathcal{E}_I / \Delta}{1 + \frac{2\nu}{N(0)\hbar\Omega_c} \exp(-\Delta/k_B T)}. \quad (4)$$

For the case of a temperature-dependent gap $\Delta(T)$, Eq.(3) will be slightly modified:

$$\left((n_{T'} - n_T) + \frac{\nu}{\hbar\Omega_c N(0)^2 \pi \Delta(T)} (n_{T'}^2 - n_T^2) \right) (\Delta(T) + k_B T/2) = \mathcal{E}_I \quad (5)$$

We approximate $n_T \simeq 2N(0)\sqrt{\pi\Delta(T)k_B T/2} \exp(-\Delta(T)/k_B T)$ ¹³ with $k_B T \ll \Delta$, resulting in a slightly modified expression for n_{pe} ¹⁵:

$$n_{pe} = \frac{\mathcal{E}_I / (\Delta(T) + k_B T/2)}{1 + \frac{2\nu}{N(0)\hbar\Omega_c} \sqrt{\frac{2k_B T}{\pi\Delta(T)}} \exp(-\Delta(T)/k_B T)}. \quad (6)$$

We note that in Eqs. (4) and (6), the explicit form of n_{pe} (and hence also $|\Delta\mathcal{A}/\mathcal{A}|$ or $|\Delta\mathcal{T}/\mathcal{T}|$) depends only on the ratio $k_B T/\Delta$, showing that the intensity of the photoresponse is a universal function of $k_B T/\Delta$ as long as the particular functional form of the temperature dependence $\Delta(T)$ is the same. Another important feature of the expressions (4) and (6) is that at $T = 0$, $n_{pe} \propto 1/\Delta(0)$, which allows a determination of $\Delta(0)$, as long as the experimental parameters required to calculate \mathcal{E}_I are recorded sufficiently precisely.

Since the decay of each phonon involves the creation of two quasiparticles, the number of high frequency phonons is proportional to the square of the number of quasiparticles $n_{T'}^2$ at temperature T' . (Taking into account conservation of energy¹⁴, at higher pulse energies when n_{pe} becomes large, we expect a crossover of the photoresponse from a linear dependence on laser power, $n_{pe} \propto I$ to a square root dependence $n_{pe} \propto \sqrt{I}$ at very high intensities.)

To enable comparison of the temperature dependences of the photoinduced transmission given by Eqs. (4) and (6) with experiments, we have plotted them as a function of temperature in Figures 2b) and c) respectively. The values for the constants for $\text{YBa}_2\text{Cu}_3\text{O}_{7-\delta}$ are: $\nu = 10-20$, $N(0) = 2.5-5 \text{ eV}^{-1}\text{spin}^{-1}\text{cell}^{-1}$, $\Omega_c = 0.1 \text{ eV}$. At low temperatures n_{pe} is essentially T -independent in both cases, falling off at higher temperatures. However, from the figure it is clear that the high-temperature behaviour is quite different in the two cases. In the case of the T -dependent gap (Fig. 2c)), the decrease in $|\Delta\mathcal{T}/\mathcal{T}|$ is much more pronounced and starts quite close to T_c at $T/T_c \approx 0.8$ dropping to zero at T_c . In the temperature-independent gap case (Fig. 2b)), the photoinduced transmission starts to drop at much lower temperatures near $T/T^* \approx 0.4$, dropping exponentially at high temperatures. Also, a notable prediction of Eq. (6) for the T -dependent gap is a small peak near $T/T_c \approx 0.7$, which is not present in the case of a temperature-independent gap formula (4).

In Fig. 2a) we have plotted the data for the photoinduced transmission amplitude for $\text{YBa}_2\text{Cu}_3\text{O}_{7-\delta}$ as a function of temperature for three different δ . Both the magnitude and the temperature dependence are seen to be strongly doping-dependent. For comparison with theory, superimposed on the theoretical curves in Figure 2 b) and c) we have plotted the normalised photoinduced reflectivity and transmission data for $\text{YBa}_2\text{Cu}_3\text{O}_{7-\delta}$ with different δ . The data for a number of underdoped samples⁵ in the range $0.15 < \delta < 0.48$ have been scaled onto a common temperature scale as suggested by the formula (4) and plotted as a function of T/T^* in Figure 2b). T^* is defined as the point where the amplitude of signal $|\Delta\mathcal{T}/\mathcal{T}|$ drops to some fixed value (for example to 5% of the maximum value). The data can be seen to fit the theoretical curve remarkably well.

For near-optimally doped $\text{YBa}_2\text{Cu}_3\text{O}_{7-\delta}$ ($\delta < 0.1$) the data are scaled by T_c and are plotted as a function of reduced temperature T/T_c . However, this time the data are superimposed on the prediction for the T -dependent BCS-like gap Eq. (6) in Figure 2c). In this case also, the fit is seen to be good, including the small maximum at $T/T_c \approx 0.7$. This maximum is particularly well observed in the data by Han et al.¹ and by Mihailovic et al.⁵, although it is not evident in the data of Stevens et al.⁴.

The experimental data thus appear to scale onto *one* of the *two* theoretical curves, the near-optimally doped $\text{YBa}_2\text{Cu}_3\text{O}_{7-\delta}$ data ($\delta < 0.1$) agreeing very well with Eq. (6) derived for a temperature-dependent gap, while the underdoped data ($\delta > 0.15$) fit expression (4) for a T -independent gap. The fact that the underdoped sample data scale onto one universal curve in Figure 2b), while the near-optimally doped data scale onto the curve in Fig. 2c), is a consequence of the scaling properties of Eqs.(4) and (6) and is a rather remarkable confirmation of the theoretical model by the experiment. From the fits of the underdoped sample data, we obtain gap values of $2\Delta = (5 \pm 1)k_B T^*$ for underdoped samples and $2\Delta = (9 \pm 1)k_B T_c$ for the near-optimally doped samples, the latter in good agreement with other optical experiments^{11,16}.

Further confirmation of the model comes from the predicted linear intensity dependence in Eqs (4) and (6). In Figure 3 we plot the T -dependence of $|\Delta\mathcal{T}/\mathcal{T}|$ for near optimally doped sample ($T_c = 89\text{K}$) for three different pump intensities. The data are seen to scale linearly with intensity as shown by the insert where \mathcal{E}_I is changed over one order of magnitude. (Unfortunately, measurements over a larger range of intensities were not possible because of steady-state laser heating.)

B. Anisotropic gap with nodes

If the gap is anisotropic and contains nodes on the Fermi surface - such as for d -wave or strongly anisotropic s -wave pairing - there is no clear gap in the spectrum. Nevertheless the quasiparticle DOS still has a strong energy dependence and a separation of low and high energy quasiparticles still exists, albeit is less pronounced than in the isotropic case. For an anisotropic gap with nodes we can approximate the quasiparticle DOS as a function of energy ε as:

$$N(\varepsilon) = N(0) \left(\frac{\varepsilon}{\Delta_a} \right)^\eta \quad (\varepsilon \ll \Delta_a), \quad (7)$$

where Δ_a is a characteristic energy scale separating the low and high-energy QPs, and the exponent η depends on the topology of the nodes on the Fermi surface. For a two dimensional Fermi surface (with nodes) $\eta = 1$, while for a 3-dimensional case $\eta = 2$.

Using equation (7) we can estimate the average energy accumulated by quasiparticles after each laser pulse:

$$\Delta E = 2FN(0)(k_B T'^{(\eta+2)} - k_B T^{(\eta+2)})/\Delta_a^\eta = \mathcal{E}_I \quad (8)$$

$$F = \int_0^\infty \frac{x^{\eta+1}}{\exp(x) + 1} dx \quad (9)$$

$F = 1.80$ for $\eta = 1$, and $F = 5.68$ for $\eta = 2$, and T' and T are the QP temperature and lattice temperatures respectively. At low temperatures, the phonon contribution to the total energy is exponentially small (Eq.(8)) and can be neglected. In this case, the high and low energy phonons are separated by an energy scale of the order of Δ_a . (Note that in general Δ_a scales with the gap, but is not equal to the amplitude of the gap.)

Solving Eq.(8) with respect to the QP temperature T' we obtain:

$$T' = \left[\frac{\mathcal{E}_I \Delta_a}{2FN(0)} + k_B T^{(\eta+2)} \right]^{1/(\eta+2)}. \quad (10)$$

The number of thermally excited quasiparticles is determined by the equation:

$$n_T = 2GN(0)k_B T^{(\eta+1)} / \Delta_a^\eta, \quad (11)$$

where G is given by the Eq.(9), except that $\eta + 1$ is replaced by η , so $G = 0.82$ for $\eta = 1$ and $G = 1.80$ for $\eta = 2$. Combining the two equations (10) and (11), we derive the following equation for the number of photogenerated quasiparticles as a function of temperature:

$$n_{pe} = \frac{2GN(0)k_B T^{(\eta+1)}}{\Delta_a^\eta} \left[\left(1 + \frac{\mathcal{E}_I \Delta_a^\eta}{2FN(0)k_B T^{(\eta+2)}} \right)^{\frac{\eta+1}{\eta+2}} - 1 \right], \quad (12)$$

The expression for the photoinduced carrier density Eq.(12) is plotted in Figure 4 with $\eta = 2$ (solid line) and the same values of $N(0)$ and \mathcal{E}_I as before. Instead of an exponential fall-off with increasing temperature, the photoexcited quasiparticle number decreases rapidly well below T_c according to a power law. In the 2-dimensional case with $\eta = 1$, (and the same parameters), the temperature dependence is shown by the dashed line in Figure 4 and differs only at the lowest temperatures. Using a T -dependent gap (e.g. of BCS form) in Eq. (12), the curve for n_{pe} is virtually indistinguishable from the case where Δ_a^η is temperature-independent. The reason for this is that the effect of the T -dependent gap is only important as $T \rightarrow T_c$, but there n_{pe} is already small.

At low temperatures we can neglect the 1 in the round brackets and obtain:

$$n_{pe} = \frac{2GN(0)}{\Delta_a^\eta} \left[\left(\frac{\mathcal{E}_I \Delta_a^\eta}{2FN(0)} \right)^{\frac{\eta+1}{\eta+2}} - k_B T^{(\eta+1)} \right]. \quad (13)$$

A feature of the d -wave model - which is particularly important for comparison with experiment - is the peculiar sub-linear behaviour of n_{pe} with laser pump intensity, $n_{pe} \sim \mathcal{E}_I^{\frac{\eta+1}{\eta+2}}$ at low temperatures. In the high temperature limit on the other hand we can expand the term in brackets to obtain a crossover to linear behaviour, with a temperature-dependent slope:

$$n_{pe} = 2G \frac{\mathcal{E}_I}{k_B T} \frac{\eta+1}{\eta+2} \quad (14)$$

It should be pointed out that in the high temperature limit, the phonon contribution should become increasingly important and the decrease of the number of photogenerated QP will eventually become exponential, just as in the case of an isotropic gap.

The data for the temperature dependence of the induced transmission for underdoped and optimally doped $\text{YBa}_2\text{Cu}_3\text{O}_{7-\delta}$ are also plotted on Figure 4, superimposed with the predicted response for the d -wave case. Clearly the T -dependence data cannot be described using a *pure* d -wave gap irrespective of dimensionality or the form of temperature dependence of $\Delta(T)$ (Eq.(12)). The linear intensity dependence shown in Fig. 3 is consistent with this observation, and is also not consistent with a d -wave gap, which predicts a sub-linear response. We note that although the data apparently exclude the possibility of a *pure* d -wave gap in underdoped and near-optimally doped YBCO, it does not entirely rule out a mixed symmetry gap with some d -wave admixture.

V. THE QUASIPARTICLE RELAXATION RATES.

As discussed in the section III, the relaxation rate of the photoinduced QPs is dominated by the energy transfer from high-frequency phonons with $\hbar\omega > 2\Delta$ to phonons with $\hbar\omega < 2\Delta$. To describe the relaxation of nonequilibrium quasiparticles in this case we consider the kinetic equation for phonons, taking into account phonon-phonon scattering¹⁷:

$$\frac{\partial n_\omega}{\partial t} = I_{ph-ph}\{n_\omega\} \quad (15)$$

where phonon-phonon scattering integral has the form:

$$\begin{aligned} I_{ph-ph}\{n_\omega\} = 2\pi \sum_{q_1, q_2} |w_{q_1, q_2}|^2 & \left\{ \frac{1}{2} [(n_\omega + 1) n_{\omega_1} n_{\omega_2} - n_\omega (n_{\omega_1} + 1) (n_{\omega_2} + 1)] \delta(\omega - \omega_1 - \omega_2) \right. \\ & \left. + [(n_\omega + 1) (n_{\omega_1} + 1) n_{\omega_2} - n_\omega n_{\omega_1} (n_{\omega_2} + 1)] \delta(\omega_2 - \omega - \omega_1) \right\}, \end{aligned} \quad (16)$$

w_{q_1, q_2} is the anharmonic coupling constant and n_ω is the phonon distribution function. (Conservation of the phonon momentum is not relevant because of umklapp scattering.) We neglect the *electron-phonon* scattering integral, because at normal temperatures the relative contribution of quasiparticles to the relaxation of phonons is small due to the relatively small number of quasiparticles compared to the phonons $N(0)\Omega_c \ll \nu$. Electron-phonon collisions can play an important role only at temperatures $T' \ll T_c$ but since - as shown in the previous section - n_{pe} is nearly constant at low temperature, T' cannot be small. The distribution function Eq.(1) reduces to 0 the parts of the collision integral Eq.(16) which describe the scattering of high and low frequency phonons separately. Only the part of the collision integral that does not conserve the number of phonons with $\omega < 2\Delta$ differs from zero.

To estimate the relaxation time, we multiply Eq. (15) by ω_q and sum over q , satisfying the condition $0 < \omega_q < 2\Delta(T)$:

$$\frac{\partial E_<}{\partial t} = \sum_{q(\omega_q < 2\Delta)} \hbar\omega_q I_{ph-ph}\{n_\omega\}. \quad (17)$$

If we suppose that the coupling constant is momentum independent $w_{q_1, q_2} = w$, then:

$$\begin{aligned} \sum_{q(\omega_q < 2\Delta)} \omega_q I_{ph-ph}\{n_\omega\} = 2\pi w^2 \int_0^{2\Delta} \omega \rho(\omega) d\omega \int \frac{1}{2} & \\ & [(n_\omega + 1) n_{\omega'} n_{\omega-\omega'} - n_\omega (n_{\omega'} + 1) (n_{\omega-\omega'} + 1)] \rho(\omega') \rho(\omega - \omega') + \\ & [(n_\omega + 1) (n_{\omega'} + 1) n_{\omega+\omega'} - n_\omega n_{\omega'} (n_{\omega+\omega'} + 1)] \rho(\omega') \rho(\omega' + \omega) \} d\omega' \end{aligned} \quad (18)$$

here $\rho(\omega) = 3\nu\omega^2/\Omega_c^3$ is the phonon density of states in the Debye approximation. We restrict ourselves to a discussion of the relatively high temperature limit where the phonon distribution function can be replaced by $k_B T/\hbar\omega$. The energy accumulated by the phonons with $\hbar\omega < 2\Delta$ is:

$$E_< = \int_0^{2\Delta} n_\omega \rho(\omega) \hbar\omega d\omega = \frac{8\nu k_B T \Delta^3}{(\hbar\Omega_c)^3} \quad (19)$$

In the integral Eq.(18) the first term is equal to 0, because it has only phonon distribution functions with $\hbar\omega < 2\Delta$. The first non-zero contribution describes the decay of the phonon with $\hbar\omega > 2\Delta$ to two phonons with $\hbar\omega < 2\Delta$:

$$I_1 \simeq \frac{13}{12} \pi w^2 \left(\frac{3\nu}{(\hbar\Omega_c)^3} \right)^3 k_B^2 T (T' - T) (2\Delta)^7 \quad (20)$$

The second contribution describes the inelastic scattering of high frequency phonon with creation of one low frequency phonon with $\omega < 2\Delta$:

$$I_2 \simeq \frac{8}{3} \pi w^2 \left(\frac{3\nu}{(\hbar\Omega_c)^2} \right)^3 k_B^2 T' (T' - T) \Delta^4 \quad (21)$$

Eq.(21) shows that the inelastic scattering of high frequency phonons is dominant in the energy relaxation of the energy if $\Delta \ll \hbar\Omega_c$ and we can neglect I_1 .

Taking into account Eqs.(17), (19-21) we obtain expressions describing the relaxation of the equilibrated QP-phonon temperature:

$$\frac{\partial T}{\partial t} = \frac{1}{\tau_{ph}}(T' - T) \quad (22)$$

$$\frac{1}{\tau_{ph}} = \frac{9\pi\nu^2w^2k_BT'\Delta(T)}{(\hbar\Omega_c)^3} \quad (23)$$

Note that Eq.(22) is rather similar to that derived by Allen¹⁰ for the temperature relaxation in the electron-phonon system in the normal metals, except that Eq.(22) describes the phonon energy relaxation modified by the gap in the quasiparticle spectrum.

The phonon-phonon relaxation time (Eq.23) can be expressed in terms of an experimental parameter, namely the Raman phonon linewidth Γ_ω . Using the Fermi golden rule we can calculate Γ_ω for $k_BT \ll \hbar\omega$:

$$\Gamma_\omega = 2\pi w^2 \sum_{q,\nu,\nu'} (n_{\omega_{q,\nu}} + 1) (n_{\omega_{-q,\nu'}} + 1) \delta(\omega_{q,\nu} + \omega_{-q,\nu'} - \omega) \simeq \frac{3\pi w^2 \nu^2 \omega^2}{4\hbar\Omega_c^3}. \quad (24)$$

The phonon relaxation rate can thus be expressed in terms of Γ_ω in the following form:

$$\frac{1}{\tau_{ph}} = \frac{12\Gamma_\omega k_BT'\Delta(T)}{\hbar\omega^2} \quad (25)$$

For a temperature dependent gap Δ , the relaxation time is expected to show a divergence $\tau_{ph} \propto 1/\Delta(T)$ as is indeed observed in optimally doped cuprates^{1,5,9,18}. A similar divergence of the relaxation time has been calculated previously by Schmidt and Schön¹⁹ and Tinkham²⁰, albeit for somewhat differently created nonequilibrium situations.

The typical relaxation timescale τ_{ph} given by the formula Eq.(25) is very close to the experimentally observed values. From the data on the Raman linewidth of the A_{1g} -symmetry apical O(4) phonon mode in YBCO - which has been shown to be particularly anharmonic - $\Gamma_\omega \approx 13 \text{ cm}^{-1}$ and $\omega \simeq 400 \text{ cm}^{-1}$ ²¹. At $T' \simeq T = T_c/2$, and using $\Delta_{T_c/2} \approx 200 \text{ cm}^{-1}$ we obtain $\tau_{ph} = 0.8 \text{ ps}$.

At low temperatures the quasiparticle temperature T' is much higher than the lattice temperature T and the formula is expected to fail. However, from the experiments (Figure 2) we see from the temperature dependence of $|\Delta T/T|$ that the number of photogenerated quasiparticles is nearly constant at low T . T' can therefore be estimated from the equation:

$$n_{T'} - n_T = \mathcal{E}_I/\Delta(0) \quad (26)$$

Taking into account that $n_T \simeq 2N(0)\Delta(0) \exp(-\Delta(T)/k_BT)$ we obtain:

$$k_BT' \simeq \Delta(T) / \ln \{1/(\mathcal{E}_I/2N(0)\Delta(0)^2 + \exp(-\Delta(T)/k_BT))\} \quad (27)$$

At low T , the nonequilibrium temperature $T' \simeq \Delta(T) / \ln \{(2N(0)\Delta(0)^2/\mathcal{E}_I\} \simeq T_c/2$, while in the high temperature limit, the exponent in the logarithm becomes large and $T' \simeq T$. Combining Eq.(25) and Eq.(27) we obtain an expression for the QP relaxation time as a function of lattice temperature T and photoexcitation energy \mathcal{E}_I which is valid for all temperatures $0 < T < T_c$:

$$\frac{1}{\tau_{ph}} = \frac{12\Gamma_\omega \Delta(T)^2}{\hbar\omega^2 \ln \{1/(\mathcal{E}_I/2N(0)\Delta(0)^2 + \exp(-\Delta(T)/k_BT))\}}. \quad (28)$$

To enable comparison of this formula with experiments, we again use Raman data on high-frequency optical phonon linewidths, a value of gap frequency of 200 cm^{-1} ($2\Delta \simeq 9k_BT_c$) from the fits in Figure 2c), the same values of $N(0) = 2.2 - 5 \text{ eV}^{-1}\text{cell}^{-1}\text{spin}^{-1}$ as in section III, and a BCS function for $\Delta(T)$. \mathcal{E}_I was again calculated using an incident laser energy of 0.2 nJ incident on a 100 nm thick film with a spot size of $\sim 100 \mu\text{m}$ diameter. We obtain a temperature dependence of the relaxation time τ_{ph} as shown in Figure 5. A comparison of the theory with the data for optimally doped $\text{YBa}_2\text{Cu}_3\text{O}_{7-\delta}$ samples^{1,5} in Figure 5 shows good agreement with the theory²² with *no adjustable*

parameters, especially near T_c . Some experimental data in the literature^{1,23} show an upturn in relaxation time at low temperatures, which is also weakly present in the data in Fig. 5. Although Eq.(28) is derived for temperatures close to T_c , an upturn at low temperature can still be reproduced by this formula if we reduce the energy per pulse \mathcal{E}_I . (In fact in the limit of $\mathcal{E}_I \rightarrow 0$, Eq. (28) gives $\tau_{ph} \propto 1/T$ at low T .) Indeed by setting $\mathcal{E}_I/N(0)$ in Eq. (28) as an adjustable parameter, rather than inserting fixed values as we have done, the low-temperature upturn in the data can be reproduced more accurately.

To end this section we briefly make a quantitative comparison of the relaxation rates for a gapped and gapless material. Comparing the relaxation time for the case of a gapped material with relaxation time in a normal metal described by Allen's formula¹⁰ we obtain:

$$\frac{\tau_{ph}}{\tau_{e-ph}} \sim \frac{\lambda \hbar^3 \omega^4}{4\pi(k_B T)^2 \Delta \Gamma_\omega} \quad (29)$$

Inserting experimental values for ω and Γ_ω we find the anharmonic phonon decay time in a superconductor to be approximately two orders of magnitude *slower* than electron-phonon relaxation in a gapless material as $\tau_{ph}/\tau_{e-ph} \sim 60 - 200$ for $T \simeq T_c$ as expected.

The calculation was performed assuming that the rate limiting step for QP relaxation is anharmonic decay of high-energy phonons, while direct electron phonon relaxation was assumed to be small. This is now justified quantitatively by a calculation of the direct electron-phonon relaxation rate. The contribution of phonon-electron scattering to the relaxation of phonon system can be estimated by deriving the corresponding relaxation rate τ_1^{-1} using the usual electron-phonon collision integral (see Appendix):

$$\frac{1}{\tau_1} = \frac{\pi N(0) \lambda \Delta(T) \Omega_c}{2\nu} \quad (30)$$

We see that the electron-phonon relaxation rate, when compared to the phonon relaxation rate is reduced by the factor $N(0) \hbar \Omega_c / \nu \ll 1$:

$$\frac{\tau_{ph}}{\tau_1} = \frac{\pi \hbar^2 N(0) \lambda \omega^2 \Omega_c}{24\nu \Gamma_\omega k_B T'} < 1 \quad (31)$$

and can therefore be neglected. However if the number of phonon modes involved in the relaxation is significantly smaller, the ratio τ_{ph}/τ_1 may approach unity. In this case the electron-phonon collisions can also contribute to the phonon relaxation. However the temperature dependence of the relaxation rate $1/\tau_1$ is very similar to the anharmonic relaxation τ_{ph} , both being proportional to $\Delta(T)$ and so the two contributions to the relaxation may be difficult to separate experimentally. The data shown in Figure 5 are fit to τ_{ph} without any fitting parameters, so it appears to be reasonable to assume that anharmonic relaxation described by Eqs. (25) and (28) is dominant in $\text{YBa}_2\text{Cu}_3\text{O}_{7-\delta}$ near optimum doping.

VI. DISCUSSION

Near optimum doping in $\text{YBa}_2\text{Cu}_3\text{O}_{7-\delta}$ ($\delta < 0.1$) we find that the theoretical model gives a good quantitative fit to the temperature dependence of the photoinduced transmission (Figure 2c)), provided we use a temperature-dependent gap (Eq. (6)). The relatively square shape of the temperature dependence of $|\Delta\mathcal{T}/\mathcal{T}|$, the weak maximum near $T/T_c = 0.7$ and the rapid drop in the signal amplitude above this temperature is a consequence of the particular temperature dependence of the gap with the property that $\Delta(T) \rightarrow 0$ as $T \rightarrow T_c$. In underdoped YBCO on the other hand (Fig. 2b)), the temperature dependence is much weaker and can only be reproduced by the calculation using a temperature-independent gap (Eq. (4)). It is *not possible* to reproduce the temperature dependence of the optimally doped data using a temperature-independent gap and vice versa, it is not possible to describe the underdoped data with a T -dependent BCS-like gap.²⁴

A similar conclusion regarding the evolution of the gap with doping is reached on the basis of the comparison of the calculated temperature dependence of the relaxation time τ with the data. The divergence at T_c shown in Figure 5 for samples near optimum doping together with the temperature dependence of $|\Delta\mathcal{T}/\mathcal{T}|$ lead to the inescapable conclusion that there is a gap in $\text{YBa}_2\text{Cu}_3\text{O}_{7-\delta}$ with ($\delta \sim 0.1$) which closes rapidly at T_c . On the other hand, the notable *absence* of this divergence of τ for underdoped $\text{YBa}_2\text{Cu}_3\text{O}_{7-\delta}$ ($\delta > 0.15$)⁵ is consistent with the existence of a T -independent gap deduced from the temperature dependence of $|\Delta\mathcal{T}/\mathcal{T}|$.

Plotting the temperature T^* and T_c as a function of δ in Figure 6, we find that T^* drops with increasing doping in a characteristic fashion, following the so-called "pseudogap" behaviour reported by other experimental techniques²⁵⁻²⁷.

Near optimum doping, the "pseudogap" becomes observable close to T_c . Such a situation occurs in BCS superconductors where gap formation is a collective effect and Cooper pairs form simultaneously with the formation of a phase coherent collective state at T_c . However, from Figure 2c) and Figure 3 there is some evidence of remaining QP excitations above T_c even near $\delta \sim 0.1$. The T -independent "pseudogap" thus appears to be still present near optimum doping, and the BCS case is not quite realized.

The underdoped state is distinctly different, with a T -independent normal state pseudogap appearing at $T^* \gg T_c$. The changes in the photoinduced transmission $|\Delta\mathcal{T}/\mathcal{T}|$ at T^* in this case are simply a result of an increase population of pairs with decreasing temperature. Since the observed changes in $|\Delta\mathcal{T}/\mathcal{T}|$ are associated only with pairing and not phase coherence (which occurs at T_c), we see no change in $|\Delta\mathcal{T}/\mathcal{T}|$ at T_c in agreement with predictions of pre-formed pairing models of the underdoped state^{28,29}. The pseudogap in this case signifies the pair binding energy, and its value is determined by the microscopic pairing mechanism. It is to first approximation temperature independent and decreases with an inverse law with increasing carrier concentration, which is consistent with increased semi-classical (Debye-Hückel) screening between charge carriers²⁸.

Since the temperature dependence of $|\Delta\mathcal{T}/\mathcal{T}|$ is actually exponential at high temperatures (Eq.4), it is more appropriate to discuss the doping dependence of the magnitude of the energy gap Δ rather than of T^* . This avoids the somewhat arbitrary criterion for determining T^* of an asymptotic function. Such a plot of Δ versus doping δ is shown in Figure 7. As predicted on the basis of screening arguments above, Δ appears to follow an inverse law $\Delta \propto 1/x$ where $x = 0.6 - \delta$ is proportional to the carrier concentration.

The doping dependence of Δ can be independently confirmed from the same data set by plotting the low-temperature value of $|\Delta\mathcal{T}/\mathcal{T}|$ as a function of δ . As can be seen from the formulae (4,6), the value of $|\Delta\mathcal{T}/\mathcal{T}|$ at $T = 0$ is proportional to \mathcal{E}_I/Δ , from which the zero-temperature gap $\Delta_{T=0}$ can be determined. A scaled plot of $1/|\Delta\mathcal{T}/\mathcal{T}|_{T \rightarrow 0}$ as a function of doping δ in Figure 7 independently confirms the inverse relation $\Delta \propto 1/(0.6 - \delta)$. We note that the observation of an inverse law is in agreement with recent experiments on $\text{La}_{2-x}\text{Sr}_x\text{CuO}_4$ ^{30,31} suggesting that it may be a universal feature of the cuprates.

A somewhat surprising feature of the data is that they are described so well by an isotropic gap over the whole range of doping. A d -wave gap is apparently not consistent with either the temperature dependence of $|\Delta\mathcal{T}/\mathcal{T}|$ or the linear intensity dependence of $|\Delta\mathcal{T}/\mathcal{T}|$. It is also not consistent with the observation of a single exponential decay of $\Delta\mathcal{T}/\mathcal{T}$ with time, since in the d -wave case we would expect a distribution of τ s, and certainly no single divergence of τ at T_c should be observed in the d -wave case. A possible explanation for the absence of a d -wave signature is that in YBCO the gap in the bulk of the sample is more or less isotropic in contrast to the surface, where it may be more d -like³². Another possibility for the apparent discrepancy between the present optical data and, for example, Raman experiments³³ are the different weights that the matrix elements have in the probing process. In the present experiments the dipole transition matrix elements average over the whole Fermi surface (FS) weighted by areas of large electron momentum. Anisotropy of the FS is not emphasized in this case. This is different than in Raman measurements, where the electronic scattering intensity is zero for an isotropic parabolic band, and Raman intensity comes only from the anisotropic regions of the FS.

We conclude by noting that the comparison of the theoretically predicted temperature dependence of the photoinduced absorption signal amplitude and relaxation time τ with the experimental results on underdoped and optimally doped $\text{YBa}_2\text{Cu}_3\text{O}_{7-\delta}$ gives good quantitative agreement. The evolution of the gap from a temperature-independent Δ to a temperature-dependent collective gap $\Delta(T)$ is a particularly striking feature of the data as is the apparent inverse dependence of the gap magnitude with doping. Although the model calculation presented in this paper was performed with the superconducting cuprates in mind, it is quite general and can, for example, also be applied to a case of photoexcitation experiments on CDW systems or narrow gap semiconductors. It could also be extended for other non-equilibrium situations as might occur in non-equilibrium superconducting high- T_c devices for example.

VII. ACKNOWLEDGMENTS

We would like to acknowledge K.A.Müller, R.Hackl and A.S. Alexandrov for valuable comments and discussions. One of us (VVK) acknowledges support of this work by RFBR Grant 97-02-16705 and by the Ministry of Science and Technology of Slovenia.

VIII. APPENDIX

To estimate the electron-phonon relaxation rate we take into account the electron-phonon collision integral¹⁷:

$$I_{ph-e}\{n_\omega\} = -4\pi \sum_k |M_{kk'}|^2 [f_k(1-f_{k'})n_q - f_{k'}(1-f_k)(n_q+1)] \delta(\epsilon_k - \epsilon_{k'} + \omega_q)$$

$M_{kk'}$ is electron-phonon coupling constant and n_ω , f_k are phonon and electron distribution functions.

Note that we neglect coherence factors in the electron-phonon collision integral. This is a reasonable approximation for the BCS case if the characteristic energy of quasiparticles is large in comparison with the gap $T > \Delta$. For underdoped case also, the normal state gap is temperature independent and hence coherence factors are equal to 0. It is easy to show that the collision integrals satisfy the conservation energy law¹⁰:

$$2 \sum_k \epsilon_k \left(\frac{\partial f_k}{\partial t} \right) + \sum_q \omega_q \left(\frac{\partial n_\omega}{\partial t} \right) = 0.$$

To calculate electron-phonon collision integral we define "electron-phonon spectral function" $\alpha^2 F$:

$$\alpha^2 F(\epsilon, \epsilon', \Omega) = \frac{2}{N(0)} \sum_{k, k'} \left| M_{k, k'} \right|^2 \delta(\omega_q - \Omega) \delta(\epsilon_k - \epsilon) \delta(\epsilon_{k'} - \epsilon')$$

Following Allen¹⁰, we suppose that $\alpha^2 F(\epsilon, \epsilon', \Omega) \simeq \alpha^2 F(\epsilon_F, \epsilon_F, \Omega) = \alpha^2 F(\Omega)$. For the sake of simplicity we make the Debye approximation for the electron-phonon spectral function $\alpha^2 F(\Omega) = \frac{\lambda \Omega^2}{\Omega_c^2}$.

$$\sum_{q(\omega_q < 2\Delta)} \omega_q I_{e-ph}\{n_\omega\} = -2\pi N(0) \int_0^{2\Delta} \Omega \alpha^2 F(\Omega) d\Omega \int_\Delta^\infty \{(f(\epsilon) - f(\epsilon + \Omega)) n_\Omega - f(\epsilon + \Omega) (1 - f(\epsilon))\} d\epsilon \quad (A1)$$

The integral Eq.(A1) can be easily evaluated:

$$I_3 \simeq \frac{4\pi k_B N(0) \lambda \Delta^4}{\hbar^2 \Omega_c^2} (T' - T) \quad (A2)$$

Formula (A2) leads to the Eq.(30) for electron-phonon relaxation rate.

Figure 1. The normalized photoinduced transmission $\Delta\mathcal{T}/\mathcal{T}$ as a function of time delay for two different samples with a) $T_c = 53\text{K}$ and b) $T_c = 90\text{K}$, each at three different temperatures. The time-evolution of the traces was fitted (solid lines) using a model with a *single* exponential decay and a Gaussian temporal profile pump pulse.

Figure 2. a) The photoinduced transmission amplitude $|\Delta\mathcal{T}/\mathcal{T}|$ in $\text{YBa}_2\text{Cu}_3\text{O}_{7-\delta}$ as a function of temperature for three different δ : for $\delta = 0.48$ (open squares), $\delta = 0.18$ (solid triangles) and $\delta \simeq 0.1$ (open circles). b) The solid line is a plot of the photoinduced transmission amplitude as a function of temperature for a temperature-independent gap using Expression (4) as a function of T/T^* . The data points are for underdoped samples with $\delta = 0.18$ with $T_c = 77\text{ K}$ (solid triangles), $\delta = 0.32$ with $T_c = 62\text{ K}$ (open triangles), $\delta = 0.44$ with $T_c = 53\text{ K}$ (solid circles) and $\delta = 0.48$ with $T_c = 48\text{ K}$ (open squares) respectively. c) The solid line is the calculated photoinduced transmission amplitude from Eq. (6) for a temperature-dependent gap as a function of normalized temperature T/T_c and data for the near-optimally doped samples $\delta \sim 0.1$ ($T_c = 90\text{K}$) from Mihailovic et al.⁵ (open circles), Stevens et al.⁴ (open squares) and Han et al.¹ (solid triangles). Note: the original datapoints of Ref.¹ were shifted by 7K in temperature. The solid lines in a) are fits with Eq. (4) for $\delta = 0.48$ and $\delta = 0.18$, and Eq. (6) for $\delta \simeq 0.1$.

Figure 3. The T -dependence of $|\Delta\mathcal{T}/\mathcal{T}|$ for near optimally doped sample ($T_c = 89\text{K}$) for three different laser intensities. The data has been normalized with respect to the energy density per unit volume deposited by the laser pulse, \mathcal{E}_I . The insert shows low temperature $|\Delta\mathcal{T}/\mathcal{T}|$ vs. \mathcal{E}_I , where $|\Delta\mathcal{T}/\mathcal{T}|$ scales linearly with \mathcal{E}_I and $\mathcal{E}_0 = 8 \times 10^{-5}$ eV cell⁻¹spin⁻¹.

Figure 4. A plot of the temperature dependence of the photoinduced transmission amplitude (i.e. PE carrier density) for a pure d -wave gap (Eq. (12)). The solid line is for a 3D case, while the dashed line is for a 2D case using the same parameters. (The ordinate scale is the same for both curves.) The data (symbols) exhibit qualitatively different behaviour than predicted by the d -wave model, irrespective of doping δ . The data were scaled in the same way as in Fig.2. The open squares represent data for $\delta > 0.15$ while the solid squares are for $\delta < 0.1$.

Figure 5. The relaxation time τ as a function of temperature for a temperature-dependent gap (Eq. (28)). The data are for the near-optimally doped samples $\delta \sim 0.1$ ($T_c = 90\text{K}$) from Han et al.¹ (full circles) and Mihailovic et al.⁵ (open circles). Note: the data points of Han et al¹ were shifted by 7K in temperature.

Figure 6. T_c (open squares) and T^* (solid squares) as a function of δ . T^* is defined as the point where the amplitude of signal $|\Delta\mathcal{T}/\mathcal{T}|$ drops to 5% of maximum of the T -dependent signal (the T -independent contribution, which is assumed to be due to Allen relaxation is subtracted).

Figure 7. The dependence of the energy gap Δ on doping δ . The open squares correspond to values of Δ determined from fits to the data using Eqs.(4) and (6), while the solid circles are obtained by plotting the scaled magnitude of the inverse of the photoinduced transmission at low temperature, $1/|\Delta\mathcal{T}/\mathcal{T}|_{T \rightarrow 0}$. In the latter case, the data were taken in a single experimental run, with carefully controlled laser operating conditions to ensure that Δ can be compared quantitatively. The dashed line is a guide to the eye showing $\Delta \propto 1/x$ bahaviour.

¹ S.G.Han Z.V.Vardeny, K.S.Wong, O.G.Symco, G.Koren, Phys.Rev.Lett. **65**, 2708 (1990)
² J.M.Chwalek, C.Uher, J.F.Whitaker, G.A.Morou and J.A.Agostinelli, Appl.Phys.Lett. **58**, 980 (1991)
³ W. Albrecht, Th.Kruse and H.Kurz, Phys.Rev.Lett. **69**, 1451 (1992)
⁴ C.J.Stevens, D.Smith, C.Chen, J.F.Ryan, B.Podobnik, D.Mihailovic, G.A.Wagner and J.E.Evetts, Phys.Rev.Lett **78**, 2212 (1997).
⁵ D.Mihailovic, B.Podobnik, J.Demsar, G.Wagner and J.Evetts (to be published in J.Phys.Chem Sol.,1998)
⁶ I.I.Mazin, A.I.Lichtenstein, O.Jepsen, O.K.Andersen and C.O.Rodriguez, Phys.Rev.B **49**, 9210 (1994)
⁷ I.I. Mazin, Phys. Rev. Lett. **80**, 3664 (1998) and C.J.Stevens, D.Smith, C.Chen, J.F.Ryan, B.Podobnik, D.Mihailovic, G.A.Wagner and J.E.Evetts, Phys. Rev. Lett. **80**, 3665 (1998)
⁸ S.V. Chekalin et al, Phys. Rev. Lett., **67**, 3860, (1991).
⁹ S.D.Borson et al, Sol. Stat. Comm. **74**, 1305 (1990)
¹⁰ P.B.Allen, Phys.Rev.Lett. **59**, 1460 (1987).
¹¹ D.N. Basov, R.Liang, B.Dabrowski, D.A. Bonn, W.N.Hardy, T.Timus, Phys. Rev. Lett., **77**, 4090, (1996).
¹² A. Rothwarth and B.N. Taylor, Phys. Rev. Lett., **19**, 27, (1967).
¹³ A.G. Aronov and B.Z. Spivak, J. Low Temp. Phys., **29**, 149, (1977).
¹⁴ A.G. Aronov, M.A. Zelikman and B.Z. Spivak, Fiz. Tverd. Tela, **18**, 2209, (1976).
¹⁵ Solving eq.(4) numerically without the approximate formula for n_T , it can be shown that formula (6) is accurate within < 10% over the whole temperature interval.
¹⁶ Z. Schlesinger et al, Phys. Rev. Lett. **65**, 801, (1990); L.D. Rotter et al, Phys. Rev. Lett. **67**, 2741, (1991).

¹⁷ J.M.Ziman "Electrons and Phonons" (Oxford University Press, London 1960), E.M. Lifshits, L.P. Pitaevskii, "Fizicheskaya Kinetika" (Moscow, 1979).

¹⁸ G.L.Easley, J.Heremans, M.S.Meyer, G.L.Doll and S.H.Liou, Phys.Rev.Lett.**65**, 3445 (1990).

¹⁹ A. Schmidt and G. Schon, J. Low. Temp. Phys. **20**, 207, (1975).

²⁰ M. Tinkham and J. Clarke, Phys. Rev. Lett. **28**, 1366, (1972).

²¹ D.Mihailovic, K.F.McCarty and D.S.Ginley, Phys.Rev.B **47**, 8910 (1993)

²² The divergence in τ appears approximately 5-8 K below T_c . Possibly this is due to a non-uniform temperature profile within illuminated area.

²³ D.H. Reitze, A.M. Weiner, A. Inam, and S. Etemand Phys. Rev. B **46**, 14309, (1992).

²⁴ Here the term *temperature-independent gap* means that the gap does not vanish at T_c , but persists above T_c . It does not exclude the possibility of a weakly temperature dependent gap.

²⁵ J.W. Loram et al, J. Superconductivity **7**, 243 (1994), J. Loram et al, Phys. Rev. Lett **71**, 1740 (1993)

²⁶ G.V.M. Williams et al, Phys. Rev. B **51**, 16503 (1995), *ibid.* Phys. Rev. Lett. **78**, 721 (1997)

²⁷ G. Ruani and P. Ricci, Phys. Rev. B **55**, 93 (1997)

²⁸ A.S. Alexandrov and N.F.Mott, "Polarons and Bipolarons" (World Scientific, 1995), A.S. Alexandrov and N.F. Mott, High Temperature Superconductors and Other Superfluids (Taylor and Francis, London, 1994), A.S.Alexandrov, V.V.Kabanov and N.F.Mott, Phys.Rev.Lett. **77**, 4796 (1996)

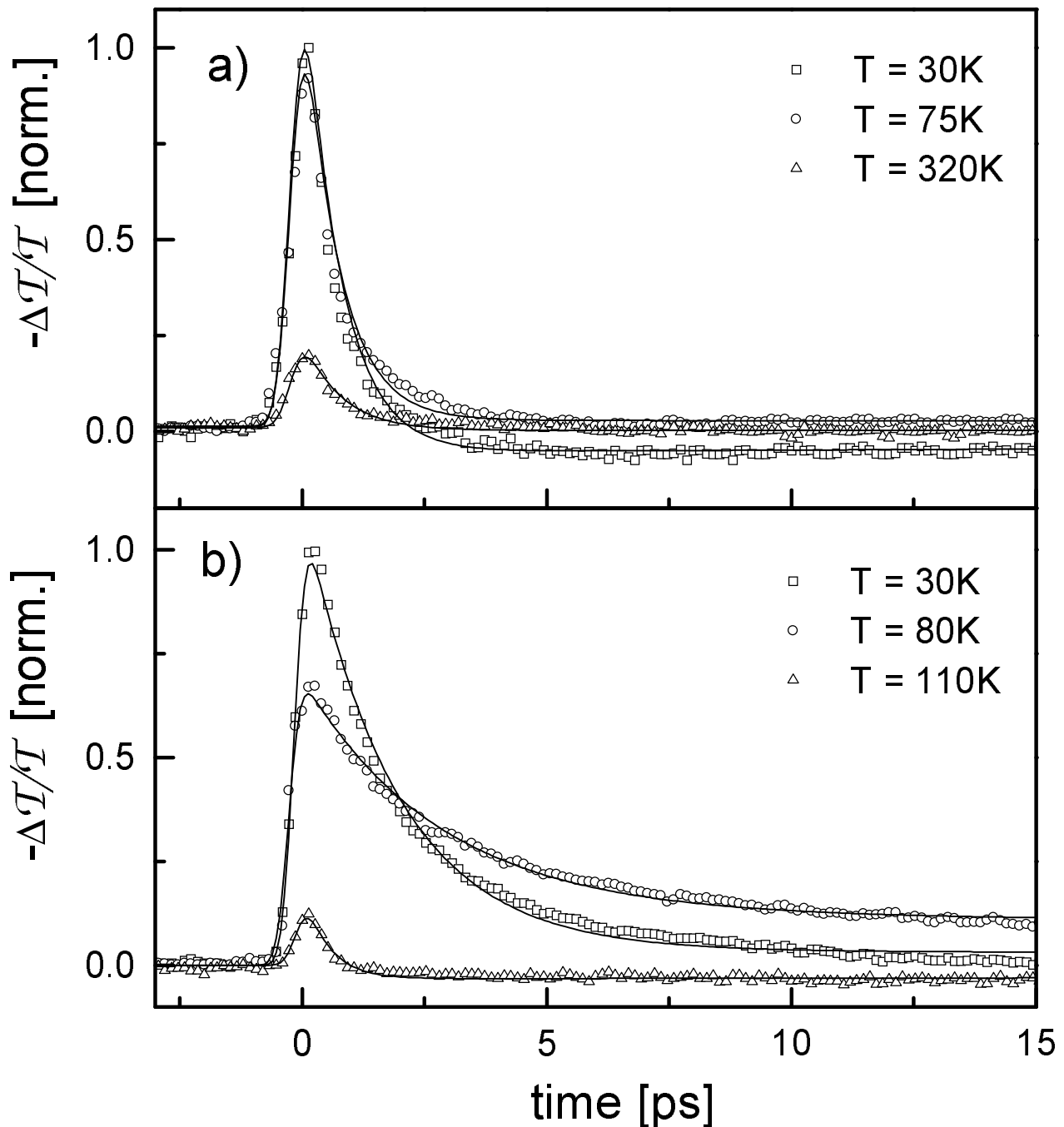
²⁹ V.J.Emery, S.A.Kivelson, and O. Zahar, Phys. Rev.B **56**, 6120 (1997), V.J. Emery and S.A. Kivelson, Nature, **374**, 434, (1995).

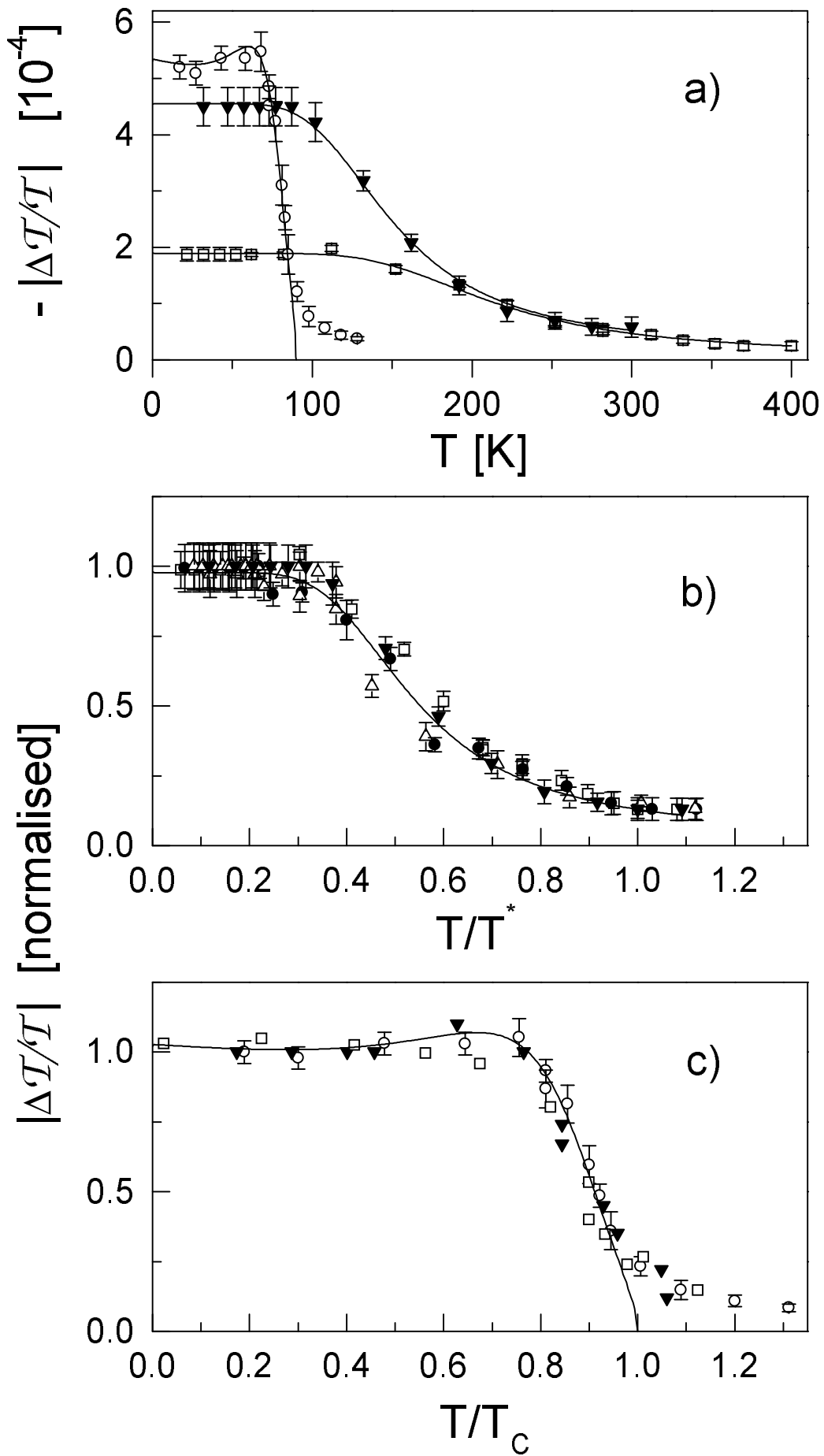
³⁰ K.A. Muller, G-M. Zhao, K. Conder, and H. Keller, J. Phys.: Condens. Matter, **10**, L291 (1998).

³¹ X.X.Bi and P.Ecklund, Phys.Rev.Lett. **70**, 2625 (1993).

³² K.A.Müller, private communication

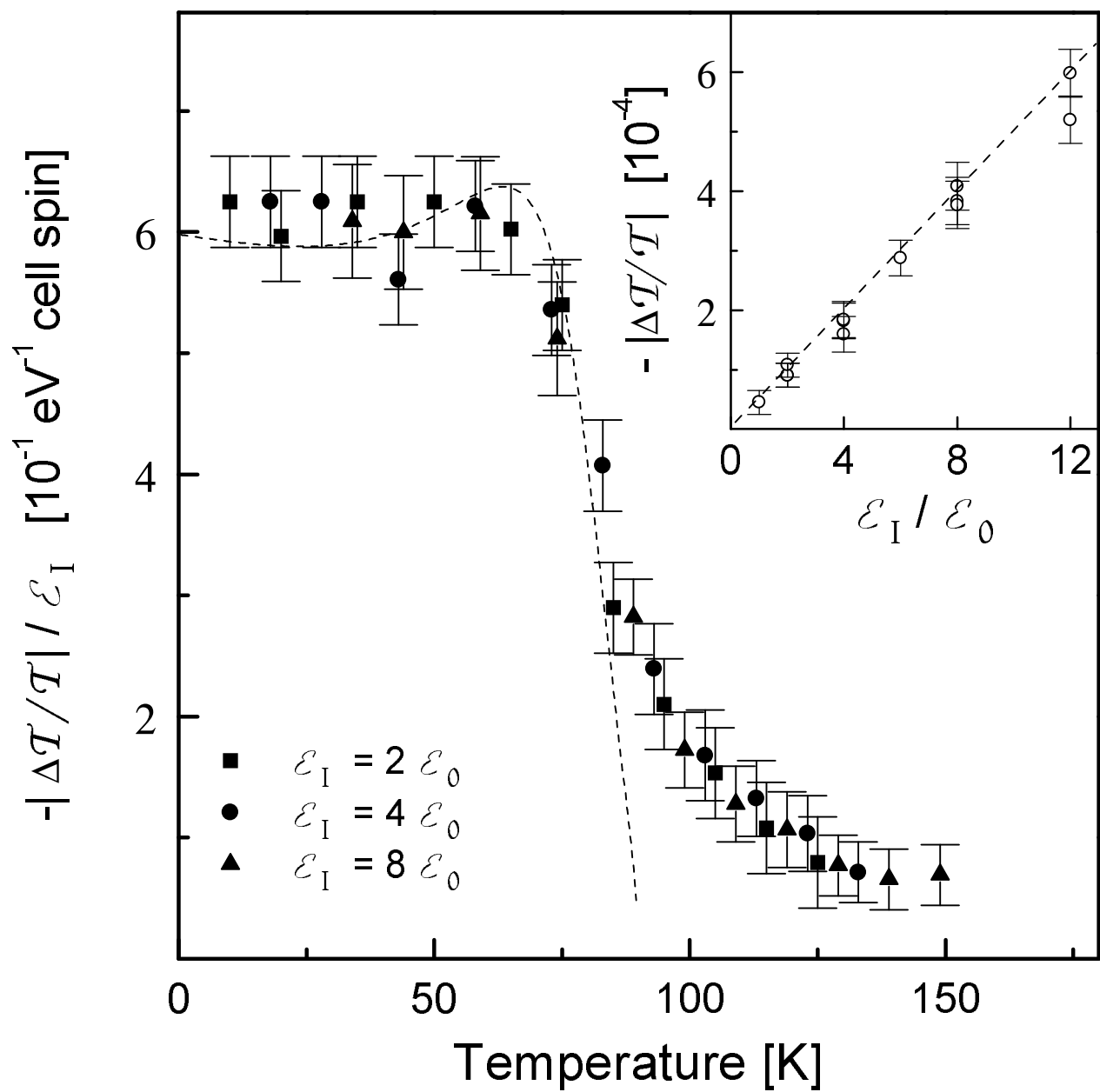
³³ R. Nemetschek et al., Phys. Rev. Lett. **78**, 4834 (1997)



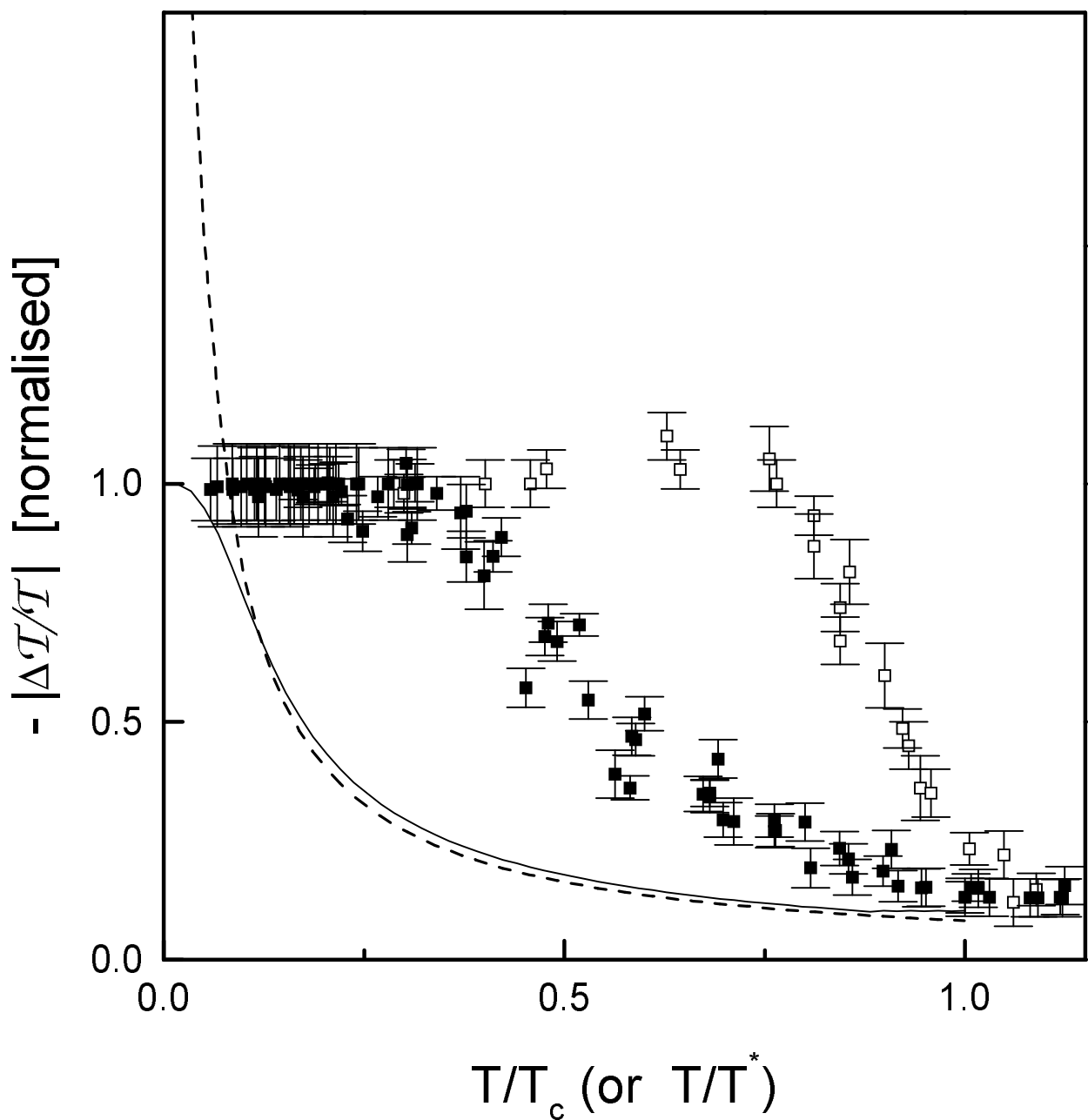


PRB 98, Figure 2

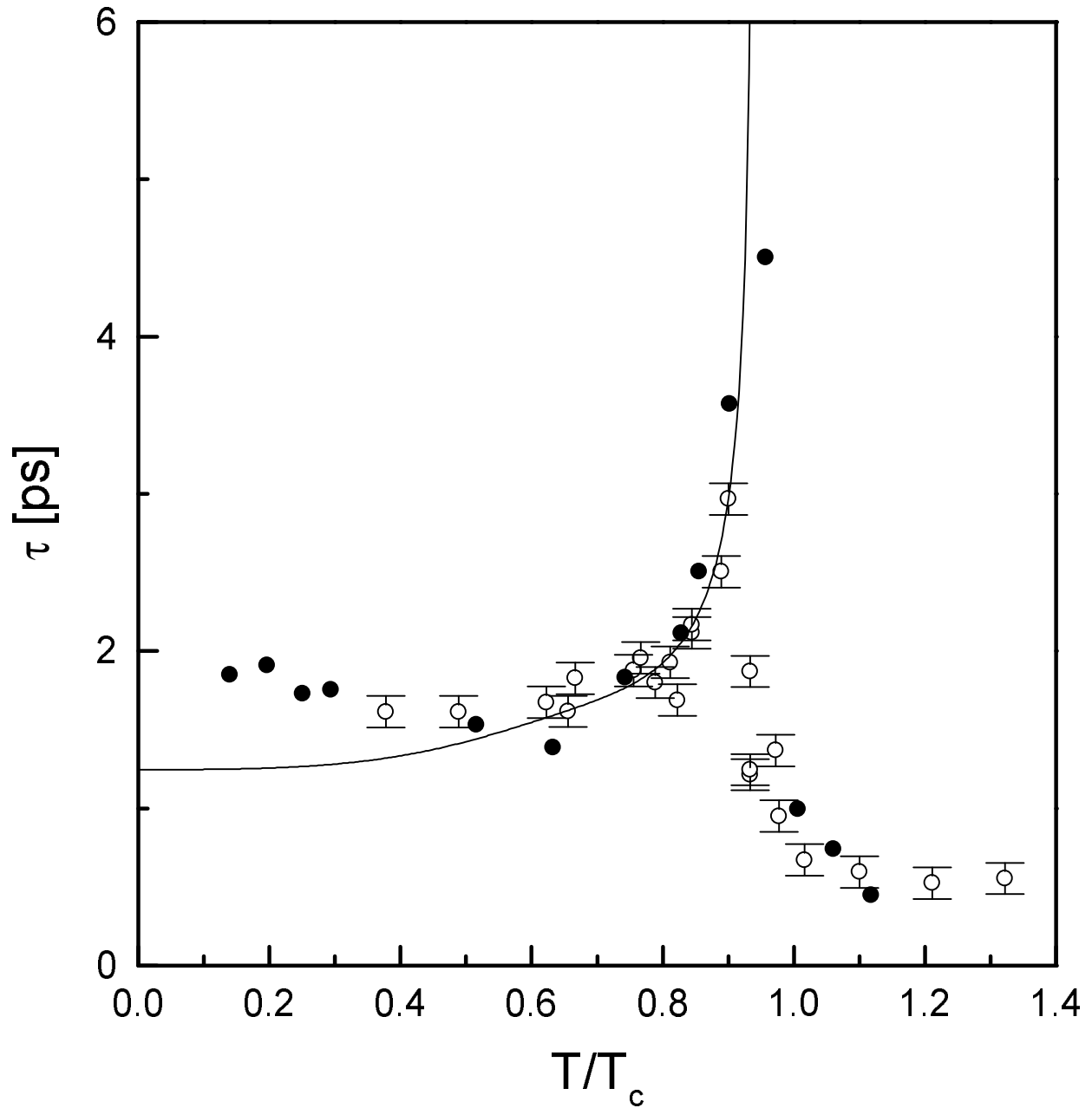
PRB 98, Figure 3



PRB98, Figure 4



PRB 98, Figure 5



PRB 98, Figure 6

